

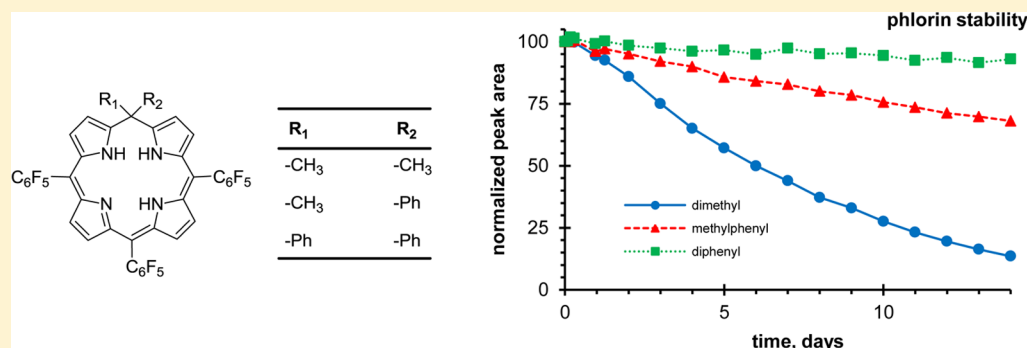
Phlorins Bearing Different Substituents at the sp^3 -Hybridized Meso-Position

Alexandra M. Bruce,[†] Emily S. Weyburne,[†] James T. Engle,[‡] Christopher J. Ziegler,^{*,‡} and G. Richard Geier, III^{*,†}

[†]Colgate University, Department of Chemistry, 13 Oak Drive, Hamilton, New York 13346, United States

[‡]Department of Chemistry, University of Akron, Akron, Ohio 44325, United States

S Supporting Information



ABSTRACT: Phlorins bearing different substituents at the sp^3 -hybridized meso-position were investigated. The extent to which different substituents at this unique position can influence phlorin spectroscopic properties, structure, and stability is of interest given that such substituents are not in direct conjugation with the phlorin macrocycle. While the effect of various substituents at the sp^2 -hybridized positions has been the subject of prior investigations, the impact of different substituents at the saturated carbon atom has not been systematically examined. In this study, phlorins with different combinations of geminal methyl and phenyl substituents were prepared in yields of 24–49% via dipyrromethane + dipyrromethanedicarbinol routes, and their NMR spectra, UV–vis spectra, X-ray crystal structures, and stability toward light and air were compared. The nature of the substituents at the sp^3 -hybridized position was found to impact spectroscopic properties, structure, and stability to varying degrees. Thus, the choice of substituents at the sp^3 -hybridized meso-position provides a further option for altering phlorin properties.

INTRODUCTION

Phlorin is a structurally interesting member of the porphyrinoid family. In addition to the typical sp^2 -hybridized meso-carbon atoms found in porphyrin, phlorin also possesses an sp^3 -hybridized meso-position. Thus, phlorin is an example of a calixphyrin—a hybrid family of molecules with structures intermediate to porphyrin and calixpyrrole (porphyrinogen).^{1,2} Additionally, the structure of phlorin is complementary to the well-known corrole system.³ While phlorin has a similar core size to porphyrin (i.e., all four meso-positions are present), the central core environment is reminiscent of corrole (i.e., the presence of three N–H groups). Unlike either porphyrin or corrole, the tetrahedral geometry of the sp^3 -hybridized carbon atom affords a nonplanar macrocycle structure.

Phlorins also display interesting properties. The presence of the sp^3 -hybridized carbon atom interrupts the main macrocycle conjugation pathway. As a result, the electronic properties of phlorin differ from porphyrin. Phlorins display a longer wavelength absorption than is typical of porphyrins. Phlorins can be oxidized by up to three electrons at modest potentials.⁴ Upon protonation, phlorins have been shown to bind

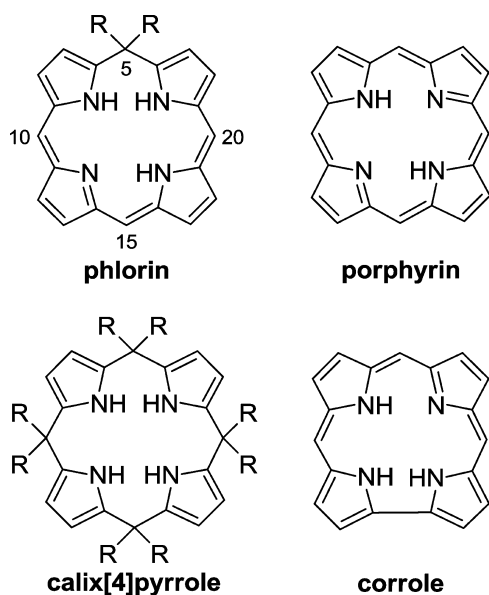
anions.^{4–6} Phlorins bearing a hydrogen atom at the sp^3 -hybridized position are tautomeric to chlorins.⁷

First identified by Woodward in the 1960s,⁸ phlorins have since been reported in a wide range of contexts.^{1,2} Yet despite past and present interest in phlorins, many phlorins suffer from poor stability toward light and air, rendering their preparation, purification, and study difficult. Phlorins bearing a hydrogen atom at the sp^3 -hybridized meso-position can readily undergo oxidation to afford an aromatic porphyrin. Phlorins geminally disubstituted at the sp^3 -hybridized position are susceptible to rapid oxidation leading to ring-opened products.⁹ Phlorin stability can be enhanced by the incorporation of substituents on one or more of the core nitrogen atoms.^{10–12} However, substitution in this way radically alters the structure of the phlorin and its coordination environment.

Several years ago, we began investigating the potential to enhance phlorin stability by the judicious incorporation of substituents at the oxidatively prone sp^2 -hybridized meso-positions. The preparation and study of phlorins bearing

Received: April 12, 2014

Published: June 11, 2014



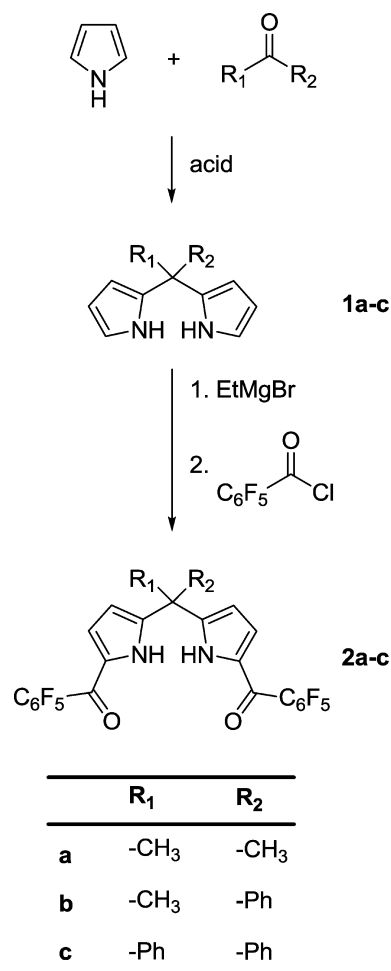
sterically bulky mesityl¹³ and electron-withdrawing pentafluorophenyl¹⁴ substituents revealed that phlorin stability could be increased and practical stability could be achieved. 5,5-Dimethyl-10,15,20-tris(pentafluorophenyl)phlorin **3a** prepared in the course of these efforts is one of the most stable free-base phlorins reported.¹⁴ Rosenthal and co-workers have utilized this phlorin in their independent studies of phlorin spectroscopy, structure, electrochemistry, and anion binding.⁴ Recently, Rosenthal and co-workers prepared and studied a series of five phlorins based on phlorin **3a** but bearing different aryl substituents at the 15-position.¹⁵ The nature of the substituent at this sp^2 -hybridized position was found to impact phlorin spectroscopic and electrochemical properties. However, a comparison of the stability of the various phlorins was not reported. Taken together, it is clear that the nature of the substituents at the sp^2 -hybridized meso-positions impacts phlorin properties and provides a means for tuning phlorin properties.

Since establishing that phlorin stability can be enhanced by the choice of substituents at the peripheral sp^2 -hybridized meso-positions, we have turned our attention to substituents at the sp^3 -hybridized position (the 5-position). The potential impact of different substituents at this location is less obvious as these substituents are not in direct conjugation with the macrocycle. To the best of our knowledge, a comparative study of phlorins differently substituted at only the 5-position has not been reported. Thus, we sought to determine whether the introduction of one or two aryl substituents at the sp^3 -hybridized meso-position (altering steric size and electronic environment) would impact phlorin spectroscopic properties, structure, and stability. Herein, we report the preparation, spectroscopic characterization (NMR and UV-vis), X-ray structural characterization, and assessment of stability of three different phlorins. Each phlorin has pentafluorophenyl groups at the sp^2 -hybridized meso-positions and bears either two methyl substituents (**3a**), a methyl and a phenyl substituent (**3b**), or two phenyl substituents (**3c**) at the sp^3 -hybridized meso-position.

RESULTS AND DISCUSSION

Preparation of Dipyrrromethanes and Diacyldipyrrromethanes. 5,5-Disubstituted dipyrrromethanes **1a–c** were

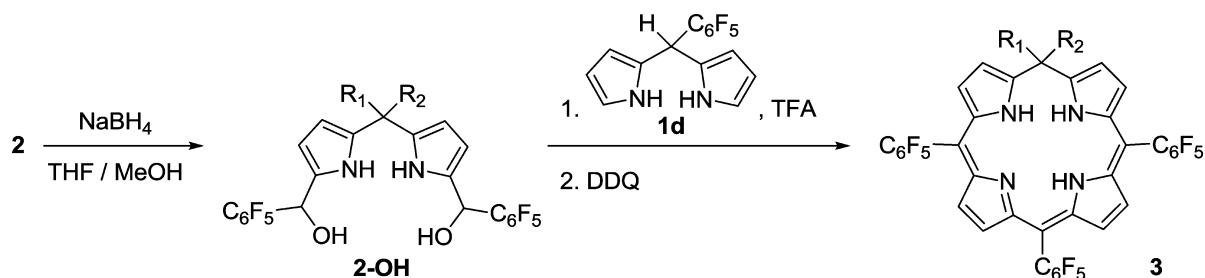
Scheme 1. Preparation of Dipyrrromethanes **1a–c** and Diacyldipyrrromethanes **2a–c**



prepared from the reaction of pyrrole with an appropriate ketone according to the literature (Scheme 1). 5,5-Dimethyldipyrrromethane **1a** was prepared using a method reported by Lindsey and co-workers.¹⁶ Dipyrrromethanes **1b**¹⁷ and **1c**¹⁸ were prepared following intriguing methods from Gambarotta and co-workers that utilized ethanol as solvent and methanesulfonic acid as the acid catalyst. We found the preparation of **1c** to be particularly convenient as analytically pure dipyrrromethane (5.1 g, 24%) crystallized directly from the crude reaction mixture as reported in the literature.¹⁸ 5-Pentafluorophenyldipyrrromethane **1d**, required for the preparation of all three phlorins, was obtained following a procedure reported by Lindsey and co-workers.¹⁹

Diacyldipyrrromethanes **2a–c** were prepared from dipyrrromethanes **1a–c** in accordance with a general procedure reported for the preparation of other diacyldipyrrromethanes (Scheme 1).²⁰ The purification of **2a** was refined from our earlier publication.¹⁴ We found that the final crystallization step takes place with better reproducibility when the crude reaction mixture is first partially purified via a short silica gel column. With this modification, we obtained 0.59 g (21% yield) compared to a variable 0.37–0.83 g (13–29% yield) from our prior method. The purification of **2b** was hampered by an inability to identify suitable conditions for crystallization. Instead, sufficient purity was obtained via two silica gel columns using different solvent systems. Evaporation of solvent

Scheme 2. Preparation of Phlorins 3a–c



diacyl DPM	R ₁	R ₂	phlorin	yield	mass
2a	-CH ₃	-CH ₃	3a	49%	206 mg
2b	-CH ₃	-Ph	3b	24%	107 mg
2c	-Ph	-Ph	3c	28%	135 mg

afforded a yellow foam that could be ground to an amorphous yellow powder (1.33 g, 35%). Modification of the general diacylation procedure was required for the preparation of **2c** due to poor solubility of **1c** in toluene. The reaction proceeded with better yield if **1c** was first dissolved in the THF solution of ethylmagnesium bromide, followed by dilution in toluene immediately prior to the addition of pentafluorobenzoyl chloride. After purification by chromatography and crystallization, **2c** was obtained in a yield similar to that of the other diacyldipyrromethanes (0.91 g, 22%).

Preparation of Phlorins. Phlorins **3a–c** were prepared in accordance with our published methodology for the preparation of phlorin **3a** (Scheme 2).¹⁴ Dipyrromethanedicarbinol species **2-OH** were prepared immediately before use by NaBH₄ reduction of **2a–c** and used without purification as reported in the literature.²⁰ Phlorins were prepared from the reaction of **2-OH** with (5-pentafluorophenyl)dipyrromethane **1d** on a 0.500 mmol scale at room temperature in CH₂Cl₂ with TFA catalysis (100 mM) followed by oxidation with DDQ. Each phlorin was isolated from polar and insoluble byproducts by passage of the crude reaction mixture through a silica pad, washing with CH₂Cl₂. Satisfactory purification of each phlorin could be achieved by passage through a neutral alumina column [CH₂Cl₂/hexanes (1:4)] followed by crystallization from CH₂Cl₂/hexanes—without need for additional silica gel chromatography as employed in our prior work.¹⁴ Each phlorin showed similar behavior during chromatography and crystallization procedures. Methodology originally developed for the preparation and purification of **3a** was not as efficient when applied to **3b** and **3c** (Scheme 2), showing that subtle changes in the nature of substituents can affect product yield in difficult to predict ways.^{20,21} Nonetheless, the isolated yields of phlorins **2b** and **2c** are typical of syntheses of porphyrinoids via dipyrromethanedicarbinol routes.^{20,22} Each phlorin was readily obtained in greater than 100 mg quantity.

NMR Analyses. ¹H NMR spectra were recorded for each phlorin. The spectra were partially assigned with the aid of ¹H–¹H COSY and NOESY spectra (see the Supporting Information for a discussion of the peak assignments). Confident assignments could be made for most peaks except for those arising from the two nonequivalent pairs of protons on the pyrrole rings furthest from the 5-position (i.e., H_{12/18} and H_{13/17}). The two signals that arise from these protons

could be determined, but not which resonance corresponds to which proton. ¹³C NMR spectra were also recorded for each phlorin in CDCl₃ (see the Supporting Information). Poor solubility of phlorin **3c** in DMSO-*d*₆ prevented comparison of ¹³C NMR spectra in that solvent.

Comparison of ¹H NMR spectra recorded in CDCl₃ is shown in Figure 1. The presence of different substituents at the sp³-hybridized meso-position impacted the chemical shifts of the β-pyrrole protons of the phlorin ring. As expected, the equivalent protons on the adjacent 3 and 7 positions were the most affected. These protons produced a signal at 6.78 ppm in **3a**. Replacement of a methyl group with a phenyl substituent in **3b** caused an upfield shift of 0.5 ppm (6.28 ppm). Replacement of both methyl groups with phenyl substituents in **3c** gave rise to a signal at an intermediate position of 6.48 ppm. Protons at positions 2 and 8 were less altered, appearing over a narrower range of 6.78 to 6.95 ppm. Interestingly, the positions of the signals due to the β-protons on the other pyrrole rings were also affected, progressively shifting upfield from **3a** to **3b** to **3c** (7.36 and 7.12 ppm; 7.29 and 7.03 ppm; and 7.06 and 6.79 ppm, respectively). Thus, different substituents at the sp³-hybridized meso-position can impact the environment of protons at some distance. Assuming similar assignments for the ¹H NMR spectra reported for four phlorins bearing different substituents at the 15-position,¹⁵ altering substituents at the 5-position had a greater effect on the NMR spectra. Across the family of phlorins bearing electron-withdrawing, electron-donating, and sterically bulky aryl substituents at the 15-position, in direct conjugation with the phlorin ring, H_{3/7} ranged from 6.77 to 6.84 ppm (0.07 ppm), H_{2/8} from 6.83 to 6.99 ppm (0.16 ppm), and H_{12/13/18/17} from 7.01 to 7.27 ppm (0.26 ppm) and 7.16 to 7.44 ppm (0.28 ppm). All of these ranges are smaller than observed across the series of phlorins **3a–c**.

¹H NMR spectra were also recorded in DMSO-*d*₆ as we had earlier observed sharper, distinct signals from the core N–H protons in this solvent.¹⁴ Different substituents at the sp³-hybridized meso-position again impacted the NMR spectra in interesting ways (Figure 2). Protons at positions 3 and 7 shifted progressively upfield from **3a** to **3b** to **3c** (6.73, 6.27, and 6.13 ppm, respectively), a range of 0.60 ppm. Once again, H_{2/8} were less impacted ranging from 7.09 to 6.96 ppm, whereas H_{12/13/18/17} were shifted upfield in **3c** relative to **3a,b** by

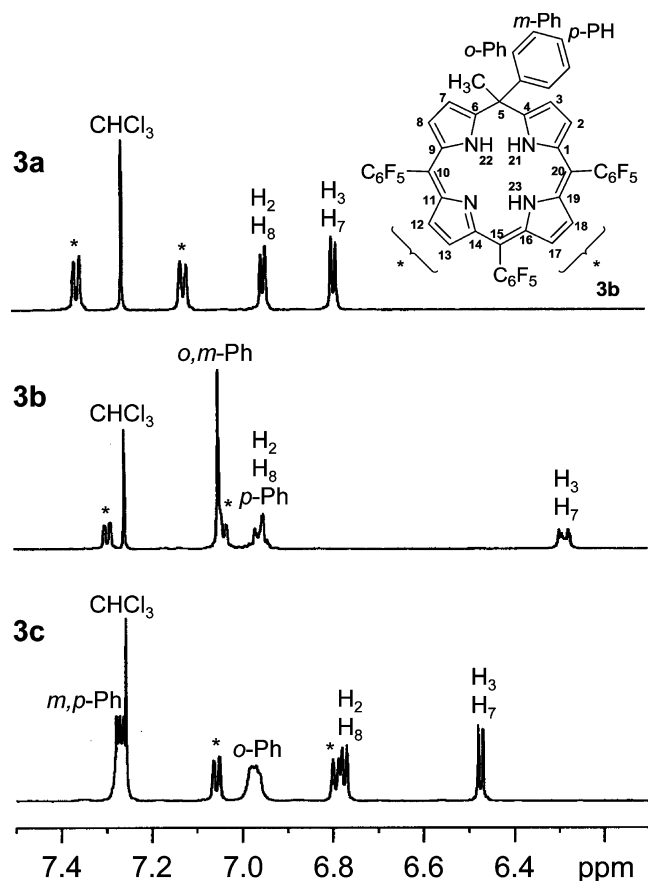


Figure 1. ^1H NMR spectra of phlorins **3a**–**c** showing an expansion of the aromatic region (CDCl_3). The numbering system is illustrated for phlorin **3b**. The peaks indicated with an asterisk (*) correspond to protons $\text{H}_{12}/\text{H}_{18}$ and $\text{H}_{13}/\text{H}_{17}$. However, the precise assignment could not be made for these two peaks.

~ 0.25 ppm for both signals. The impact of different substituents at the 5-position on the chemical shift of the N–H peaks was particularly pronounced. Proton NH_{23} was found at 6.10 and 6.11 ppm for **3a** and **3b** respectively, but appeared much farther downfield at 7.69 ppm for **3c**. A similar downfield shift was observed for $\text{NH}_{21/22}$. The signal appeared at 6.89 and 6.98 for **3a** and **3b**, respectively, but at 8.38 ppm for **3c**. Again, different substituents at the sp^3 -hybridized meso-position impact the environment of protons on the phlorin ring, even those at greater distance from the 5-position.

UV–vis Analyses. Absorption spectra for phlorins **3a**–**c** were measured in CHCl_3 (Figure 3) and toluene (see the Supporting Information). The spectra for phlorins **3a** and **3b** were nearly identical. The primary point of difference was that the longer wavelength band for **3b** was slightly blue-shifted relative to that of **3a** (647 and 653 nm, respectively, in CHCl_3 ; 651 and 654, respectively, in toluene). Spectra for phlorin **3c** differed more sharply. The longer wavelength band was red-shifted by ~ 20 nm to 667 and 674 nm in CHCl_3 and toluene, respectively. The molar absorptivity was also diminished by $\sim 20\%$ ($\sim 21000 \text{ M}^{-1} \text{ L}^{-1}$ in both solvents) relative to **3a,b** ($\sim 27000 \text{ M}^{-1} \text{ L}^{-1}$ for both compounds in both solvents). The effect on the absorption spectra of different substituents at the sp^3 -hybridized meso-position is similar to that reported for the family of phlorins bearing different substituents at the 15-position.¹⁵ In that report, the position of the longer wavelength band varied from 655 to 670 nm, a range of 15 nm. Thus,

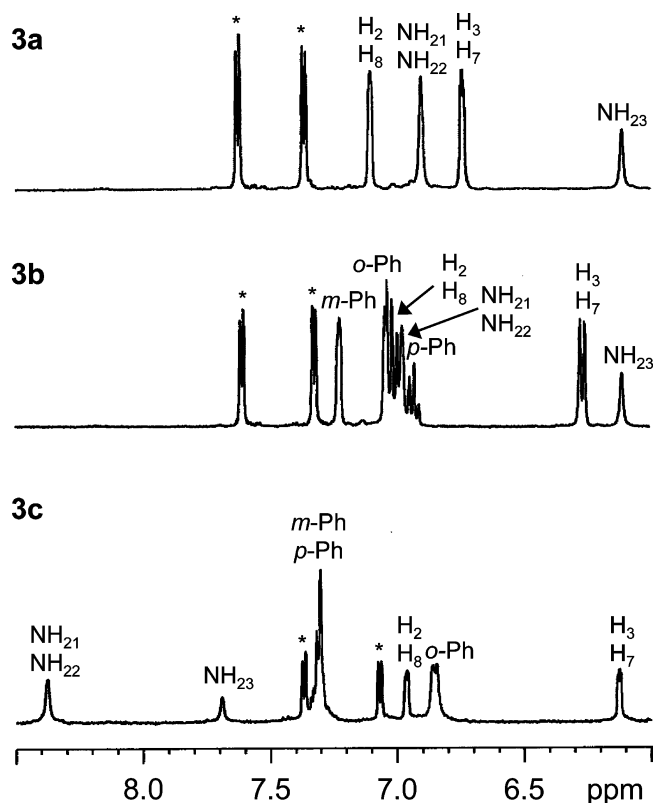


Figure 2. ^1H NMR spectra of phlorins **3a**–**c** showing an expansion of the aromatic region ($\text{DMSO-}d_6$). The numbering system is shown in Figure 1. The peaks indicated with an asterisk (*) correspond to protons $\text{H}_{12}/\text{H}_{18}$ and $\text{H}_{13}/\text{H}_{17}$. However, the precise assignment could not be made for these two peaks.

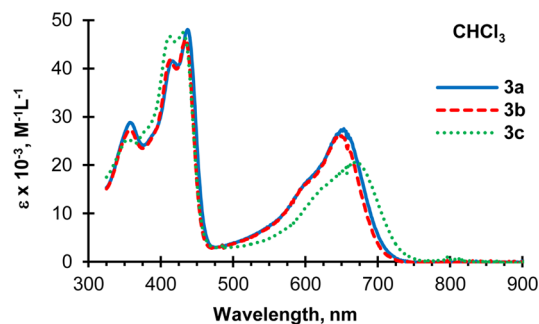


Figure 3. UV–vis spectra of dimethylphlorin **3a**, methylphenylphlorin **3b**, and diphenylphlorin **3c** in CHCl_3 .

altering substituents at the 5-position provides another option for tuning absorption properties.

Crystallographic Analyses. Phlorins **3a**–**c** were characterized by X-ray diffraction (Figure 4). X-ray data collection and structure parameters are listed in the Supporting Information. Phlorin **3a** was recently elucidated in the monoclinic space group $P2_1$.⁴ In our study, we isolated a second crystal form in the orthorhombic space group $P2_12_12_1$. The loss of conjugation caused by the presence of the sp^3 -hybridized carbon atom in the phlorin macrocycle results in nonplanar structures for phlorins **3a**–**c**, in contrast to most aromatic porphyrinoids. In phlorins **3a**–**c**, the two pyrrole units opposite the sp^3 -hybridized carbon atom are largely coplanar. However, the pyrrole rings immediately adjacent to the 5-position are puckered out of the macrocycle plane, rising above the plane

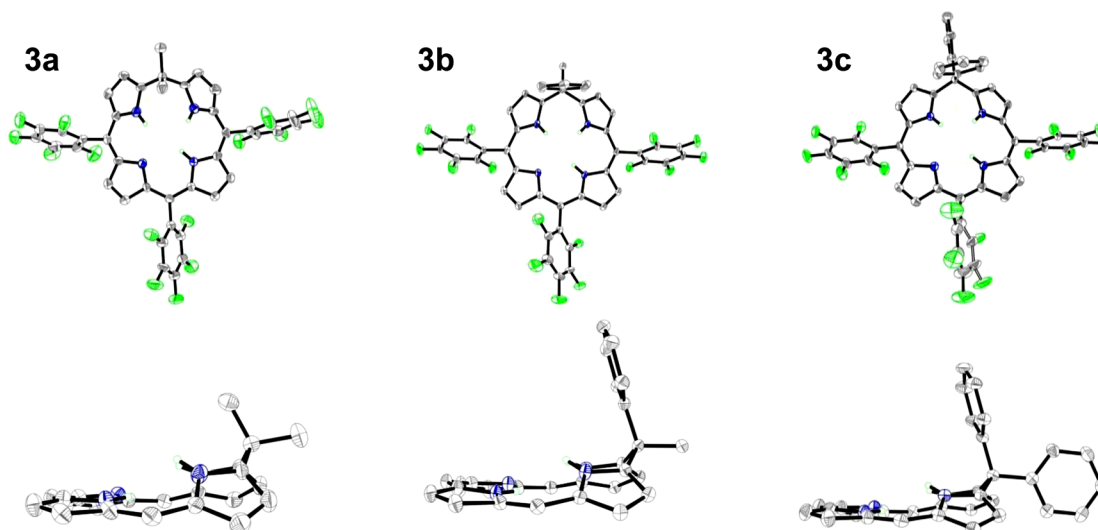


Figure 4. Top: structures of phlorins 3a–c with 35% thermal ellipsoids. Nonionizable hydrogen atoms have been omitted for clarity. Bottom: side views of phlorins 3a–c with 35% thermal ellipsoids. Perfluorophenyl groups and nonionizable hydrogen atoms have been omitted for clarity.

defined by the 11 atoms of the opposite dipyrrole unit. The substituents on the sp³-hybridized carbon atom do affect the degree of nonplanarity, but some variability is also observed, as will be discussed below.

There are only three structurally elucidated examples of phlorins in the literature, excluding core modified,²³ expanded core modified,²⁴ expanded,²⁵ or confused²⁶ phlorin systems. The first example published by Krattinger and Callot,¹¹ bears a phenyl N-substituent on one of the pyrrole nitrogen atoms adjacent to the sp³-hybridized meso-position. The bulky N-substituent causes the pyrrole to invert, such that this phlorin is not a valid structural comparison to 3a–c. In 2005, Gryko and co-workers presented the structure of a phlorin serendipitously isolated from the reaction of (5-pentafluorophenyl)-dipyrromethane with 4-nitrobenzaldehyde.²⁷ The resultant phlorin has a dipyrin and *p*-nitrophenyl group attached to the sp³-hybridized meso-position. The macrocycle deviates from planarity as observed from phlorins 3a–c. The two pyrrolic nitrogen atoms (N₂₁ and N₂₂) deviate from the plane of the dipyrrole across from the sp³-hybridized carbon atom, and the three ionizable hydrogen atoms are assigned to the pyrrole nitrogen positions immediately adjacent to the sp³-hybridized carbon position (N₂₁ and N₂₂) and to one of the opposite pyrroles (N₂₃). Notably, the deviation from planarity is less than observed from 3a–c as will be discussed below. The deviation from planarity in Gryko's phlorin structure can be assessed by measurement of the distance of the nitrogen atoms adjacent to the sp³-hybridized carbon atom (N₂₁ and N₂₂) from the plane defined by the opposite dipyrromethane unit. The phlorin bearing the dipyrin unit exhibits deviations of ~0.850 and ~0.636 Å for the two out of plane pyrrolic nitrogen atoms. The most recent phlorin X-ray crystal structure presented in the literature is for the dimethyl substituted species 3a reported by Rosenthal and co-workers.⁴ This phlorin has the same protonation state and bonding features as seen in the Gryko structure. This macrocycle is also nonplanar, with nitrogen deviations from the dipyrromethane unit of ~0.843 and ~0.801 Å.

In the structures of 3a–c determined in this study, the sp³ character of the disubstituted meso-carbon atom is readily observed in the bond lengths to adjacent atoms, all of which are

single in character. The pyrrole rings on either side of the sp³-hybridized carbon atom show electron delocalization in their carbon–carbon bonding, all indicative of localized aromaticity in these pyrrole rings. In contrast, the other rings show alternating double and single bonds with the lengths varying by more than 0.2–0.3 Å. The lone carbon–nitrogen double bond of the macrocycle (located on the deprotonated pyrrole ring, C₁₄–N₂₄) can be identified as it is the shortest carbon–nitrogen bond within the structure at ~1.34–1.36 Å. This factor, plus the electron density on the difference map, led to assignment of the three ionizable protons to the two pyrroles immediately adjacent to the sp³-hybridized carbon atom and to one of the opposite pyrrole units.

The deviation from planarity in phlorins 3a–c is variable and partially dependent on the identity of the substituents on the sp³-hybridized carbon atom. As can be seen in the side-on views in Figure 4, the 5,5-diphenylphlorin 3c shows the greatest degree of planarity, 5-methyl-5-phenylphlorin 3b is the most nonplanar, and the new crystal form of 5,5-dimethylphlorin 3a is intermediate. Phlorin 3b exhibits the largest distances, ~1.016 and ~1.017 Å, in spite of the increased steric bulk of the nearby phenyl ring. This contrasts with the diphenyl variant 3c which has the smallest distances of ~0.811 and ~0.812 Å. However, a comparison of the previously elucidated structure of 3a to the orthorhombic form indicates that packing forces play a role in the degree of planarity of the phlorins. In the orthorhombic form of 3a, the distances measure ~0.902 and ~0.923 Å, considerably longer than that seen for the monoclinic form (~0.843 and ~0.801 Å). In spite of some variability of planarity due to packing forces, the increased steric bulk of the phenyl substituents in 3c affects the geometry at the sp³-hybridized carbon atom. The phenyl–carbon–phenyl bond angle is larger (110.7°) than for an ideal tetrahedron and larger than the corresponding angles in 3a and 3b (108.5° and 108.4° respectively). The angle between the adjacent pyrrole rings is also greater in 3c compared to 3a and 3b (109.4°, 106.7°, and 107.4°, respectively). Taken together, the nature of substituents at the sp³-hybridized meso-position can impact the structure of the phlorin.

Phlorin Stability. The stability toward light and air of phlorins 3a–c in dilute solution was investigated. Similar to our

previous studies of the stability of meso-substituted corroles,²¹ octaphyrins,²⁸ phlorins bearing mesityl substituents,¹³ and phlorin **3a**;¹⁴ solutions of each phlorin were prepared in a variety of solvents, and changes in UV–vis spectra were followed as a function of time of exposure to ambient room light (i.e., light from conventional overhead fluorescent lighting). The solutions were monitored closely for 8 h of exposure, followed by monitoring once a day for a period of 2 weeks. Additionally, solutions of phlorins **3a–c** were monitored by HPLC for a period of 2 weeks of continuous exposure to light. For each solvent condition, solutions of **3a–c** were made at the same time so that changes in UV–vis spectra or HPLC peak area were monitored under identical conditions for the three phlorins.

In our initial experiments, solutions of phlorins **3a–c** were prepared in hexanes, toluene, CH₂Cl₂, THF, ethyl acetate, acetone, acetonitrile, and methanol such that the absorbance of the long wavelength peak (~650 nm) was initially ~0.7. As the molar absorptivity of **3c** at that wavelength is ~20% lower than that of **3a,b**, we also carried out analyses in a subset of solvents (toluene, CH₂Cl₂, THF, and methanol) on phlorin solutions of approximately uniform concentration (~0.025 mM). The additional experiments were done to be certain that any differences in phlorin stability were not due to differences in initial conditions.

Plots of overlaid UV–vis spectra for phlorins **3a–c** in CH₂Cl₂ recorded from solutions of uniform initial concentration over a period of 14 days of exposure to light are shown in Figure 5 (see the Supporting Information for the complete set of overlaid spectra for solutions of uniform initial absorbance and concentration for 8 h and 14 d of exposure to light). The overlaid spectra reveal gradual changes in the UV–vis spectra for each phlorin, with an apparent faster change for **3a** followed by **3b**, with **3c** appearing to be the most stable. Fairly clean isosbestic points are observed for each phlorin. These qualitative trends are evident across the solvents and initial conditions (similar absorbance or similar concentration) investigated (see the Supporting Information). Under all conditions, phlorin **3a** consistently showed the fastest spectroscopic changes. Phlorin **3c** generally showed the slowest rate of change, with the exception of THF solutions where **3b** showed a slightly more gradual change.

Comparison of changes in the UV–vis spectra as a function of exposure to light was also made by plotting absorbance as a function of time of exposure. In our earlier studies,^{13,14} we plotted change in absorbance of the peak at ~650 nm. However, in this study we observed in some solvents (most significantly acetone with **3c**) that an isosbestic point was present very close to that peak causing a likely under-reporting of absorbance change. Thus, in this study we also plotted the change in absorbance of the primary peak found at ~430 nm (see the Supporting Information for additional discussion). Figure 6 provides illustrative plots following changes at both peaks for the solutions of phlorins **3a–c** that provided the spectra shown in Figure 5 (see the Supporting Information for the complete set of plots). The apparent magnitude of the difference in phlorin stability does depend on which peak is monitored, with greater differences between **3a–c** generally observed when following the peak at shorter wavelength. However, the overall detection of differences in stability, and the general order of stability do not depend on the wavelength monitored. The initial conditions (similar absorbance or similar concentration) also did not have a significant impact on the

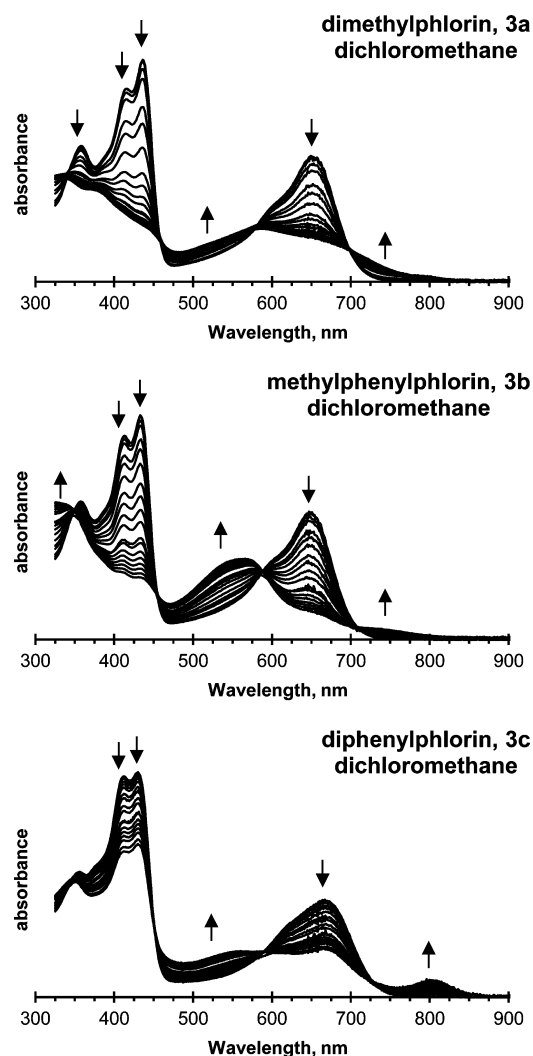


Figure 5. UV–vis spectra of CH₂Cl₂ solutions of phlorins **3a–c** recorded after exposure to light and air for 0–14 days. The arrows indicate the direction of the change.

detection of differences in stability and the general order of stability. Based on graphical representation of changes in the UV–vis spectra, phlorin **3c** is generally the most stable and **3a** is the least stable of the three phlorins.

To confirm the conclusions drawn from UV–vis analyses, analogous experiments were carried out with HPLC monitoring. Solutions of phlorins **3a–c** were prepared in toluene, CH₂Cl₂, and THF, and the area of the phlorin peak was followed over 14 days of exposure to light. An illustrative result is shown in the bottom panel of Figure 6. While a slower rate of decomposition for all three phlorins was observed in the HPLC experiments, the overall trends are in good agreement with the UV–vis findings. Phlorin **3c** shows the slowest and smallest decline in peak area over time, whereas **3a** shows the greatest changes. The overall slower rate of change for all phlorins could stem from the ~10-fold higher phlorin concentration required for HPLC monitoring. The solutions used in the HPLC experiments were noticeably darker in color which likely impacted the depth of light penetration. Comparison of methods for assessing phlorin stability and representing the data as shown in Figures 5 and 6 highlight the importance of applying multiple approaches to distinguish general trends from potential anomalies. Both UV–vis and HPLC assessment of

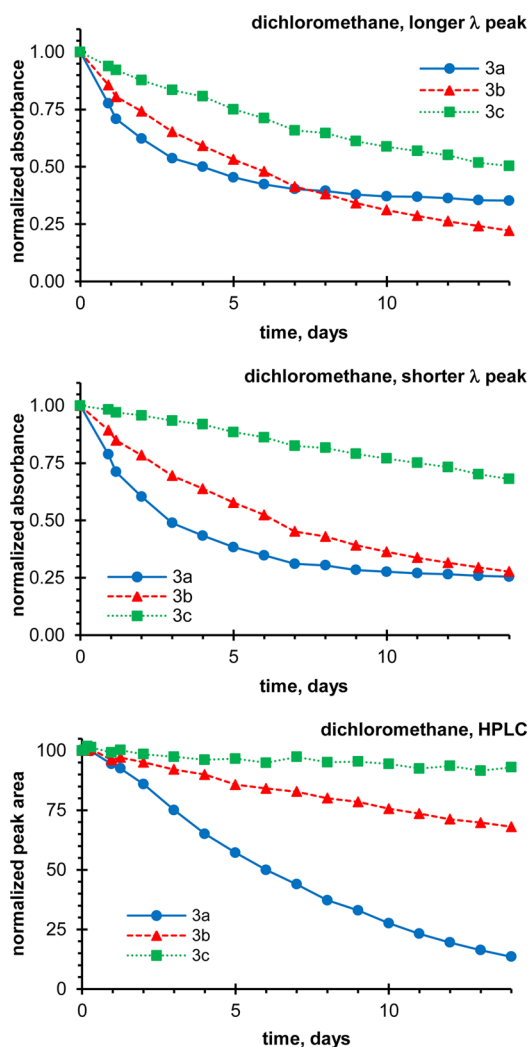


Figure 6. Plots of absorbance (top and middle panels) or HPLC peak area (bottom panel) as a function of time of exposure to light for CH_2Cl_2 solutions of phlorins **3a**–**c**. The absorbance wavelengths monitored for the top panel were 655 nm (**3a**), 650 nm (**3b**), and 674 nm (**3c**). The absorbance wavelengths monitored for the middle panel were 439 nm (**3a**), 436 nm (**3b**), and 431 nm (**3c**). The initial concentration of each phlorin sample for UV–vis monitoring was approximately the same (~ 0.025 mM), and note that the same solutions of **3a**–**c** were utilized for the two plots. HPLC monitoring (bottom panel) was performed at 434 nm (**3a**), 434 nm (**3b**), and 430 nm (**3c**). The initial concentration of each phlorin sample for HPLC monitoring was approximately the same (~ 0.30 mM).

phlorin stability revealed differences between the three phlorins. Thus, substituents at the sp^3 -hybridized meso-position can impact phlorin stability, despite not being in direct conjugation with the macrocycle.

CONCLUSION

Phlorins bearing different substituents at the sp^3 -hybridized meso-position were prepared and their NMR spectra, UV–vis spectra, X-ray crystal structures, and stability toward light and air were compared. The nature of the substituents at the sp^3 -hybridized position were found to impact spectroscopic properties, structures, and stability of the phlorins. Although not in direct conjugation with the phlorin macrocycle, the selection of substituents at the sp^3 -hybridized position provides an additional approach for altering phlorin properties. This

finding provides encouragement toward the preparation and study of additional phlorins bearing a wider array of substituents at the sp^3 -hybridized meso-position.

EXPERIMENTAL SECTION

General Experimental Methods. ^1H NMR (400 MHz), ^{13}C NMR (100 MHz), and absorption spectra were collected routinely. Melting points are uncorrected. Column chromatography was performed on silica (Merck, 230–400 mesh, 60 Å) or neutral alumina (Fisher, 80–200 mesh). THF used in the reduction of diacyl dipyrromethanes was stored over 4-Å Linde molecular sieves. Toluene used in the synthesis of diacyl dipyrromethanes was obtained from a solvent purification system. All other chemicals are reagent grade and were used as obtained. Dipyrromethanes **1a**,¹⁶ **1b**,¹⁷ **1c**,¹⁸ and **1d**¹⁹ were prepared as described in the literature.

5,5-Dimethyl-1,9-bis(pentafluorobenzoyl)dipyrromethane (2a). The reaction of 5,5-dimethyldipyrromethane **1a** (0.871 g, 5.00 mmol) with ethylmagnesium bromide (25.0 mL, 250 mmol, 1 M in THF) in dry toluene (100 mL) under argon, followed by addition of a solution of pentafluorobenzoyl chloride (1.80 mL, 12.5 mmol) in dry toluene (12.5 mL) was carried out as described in the literature.²⁰ Purification of **2a** from the crude reaction mixture was refined from our earlier publication,¹⁴ and was carried out as follows. The crude reaction mixture was subjected to chromatography [silica gel, CH_2Cl_2 followed by $\text{CH}_2\text{Cl}_2/\text{EtOAc}$ (25:1)]. The diacyl dipyrromethane eluted quickly after the increase in solvent polarity, and afforded a light yellow solid (774 mg) upon evaporation of the solvent. The diacyl dipyrromethane was further purified by crystallization from CH_2Cl_2 /hexanes with gradual evaporation of the CH_2Cl_2 over ~ 1 h at $\sim 45^\circ\text{C}$ yielding a white crystalline solid (21%, 586 mg). Melting point and ^1H NMR analyses were consistent with published values.¹⁴ Anal. Calcd for $\text{C}_{25}\text{H}_{12}\text{F}_{10}\text{N}_2\text{O}_2$: C, 53.40; H, 2.15; N, 4.98. Found: C, 53.45; H, 2.14; N 5.08.

5-Methyl-5-phenyl-1,9-bis(pentafluorobenzoyl)-dipyrromethane (2b). Following a general diacylation procedure from the literature,²⁰ ethylmagnesium bromide (30.0 mL, 300 mmol, 1 M in THF) was added dropwise over 15 min to a solution of 5-methyl-5-phenyldipyrromethane **1b** (1.42 g, 6.00 mmol) in dry toluene (120 mL) under argon. The reaction mixture was stirred for 30 min at room temperature, and a solution of pentafluorobenzoyl chloride (2.16 mL, 15.0 mmol) in dry toluene (15 mL) was added dropwise over 10 min. The reaction mixture was stirred for 30 min at room temperature. The reaction was quenched by addition of a saturated aqueous NH_4Cl (90 mL). The organic layer was separated and washed with water (60 mL) and then brine (60 mL) followed by drying over Na_2SO_4 . The crude product mixture was concentrated yielding a golden foam. The crude reaction mixture was subjected to chromatography [silica gel, CH_2Cl_2 /hexanes (2:1) followed by CH_2Cl_2]. The diacyl dipyrromethane eluted quickly after the increase in solvent polarity and afforded a light green foam (1.98 g) upon evaporation of the solvent. Attempts to further purify **2b** by crystallization or precipitation were not successful. Thus, the sample was subjected to further chromatography [silica gel, hexanes followed by hexanes/ EtOAc (20:1)]. Evaporation of solvent and drying under vacuum yielded a yellow foam which was ground to an amorphous yellow powder (35%, 1.33 g): ^1H NMR (CDCl_3 , 400 MHz) δ 9.33 (s, 2H), 7.36 (m, 3H), 7.13 (m, 2H), 6.68 (m, 2H), 6.16 (dd, $J = 2.7, 4.0$ Hz, 2H), 2.17 (s, 3H); $^{13}\text{C}\{^1\text{H}\}$ NMR (CDCl_3 , 100 MHz) δ 28.2, 45.6, 111.3, 113.7 (t, $J = 20$ Hz), 121.8, 127.1, 128.1, 129.1, 131.2, 137.6 (d, $J = 256$ Hz), 142.3 (d, $J = 264$ Hz), 143.2, 144.0 (d, $J = 250$ Hz), 146.4, 172.1; HRMS (ESI-TOF) m/z [M + H] calcd for $\text{C}_{30}\text{H}_{14}\text{F}_{10}\text{N}_2\text{O}_2\text{H}$ 625.0974, found 625.0975; IR ν_{max} (thin film)/ cm^{-1} 1615.

5,5-Diphenyl-1,9-bis(pentafluorobenzoyl)dipyrromethane (2c). Ethylmagnesium bromide (30.0 mL, 300 mmol, 1 M in THF) was added dropwise over 15 min to 5,5-diphenyldipyrromethane **1c** (1.79 g, 6.00 mmol) under argon. [Note: it is important for this specific reaction that the ethylmagnesium bromide solution is added to the dipyrromethane prior to adding the toluene solvent as the dipyrromethane dissolves poorly in toluene leading to a very low level

of acylation.] The reaction mixture was stirred for 30 min at room temperature. Dry toluene (120 mL) was added, immediately followed by the dropwise addition of a solution of pentafluorobenzoyl chloride (2.16 mL, 15.0 mmol) in dry toluene (15 mL) over 10 min. The reaction mixture was stirred for 30 min at room temperature. The reaction was quenched by addition of a saturated aqueous NH_4Cl (90 mL). The organic layer was separated and washed with water (60 mL) and then brine (60 mL) followed by drying over Na_2SO_4 . The crude product mixture was concentrated, yielding an orange-brown film. The crude reaction mixture was subjected to chromatography [silica gel, CH_2Cl_2 /hexanes (1:1) followed by CH_2Cl_2 /hexanes (2:1)]. The diacyldipyrromethane eluted quickly after the increase in solvent polarity and afforded a light yellow-green film (1.88 g) upon evaporation of the solvent. The diacyldipyrromethane was further purified by crystallizing twice from CH_2Cl_2 /hexanes with gradual evaporation of the CH_2Cl_2 over ~1 h at ~50 °C yielding a light yellow crystalline solid (22%, 0.911 g): mp 218–219 °C; ^1H NMR (CDCl_3 , 400 MHz) δ 9.12 (s, 2H), 7.40 (m, 6H), 7.10 (m, 4H), 6.71 (m, 2H), 6.22 (dd, $J = 2.7, 4.0$ Hz, 2H); $^{13}\text{C}\{^1\text{H}\}$ NMR (CDCl_3 , 100 MHz) δ 56.7, 113.6 (t, $J = 21$ Hz), 113.8, 121.3, 128.4, 129.0, 129.1, 131.0, 137.6 (d, $J = 256$ Hz), 141.9, 142.4 (d, $J = 255$ Hz), 143.9 (d, $J = 252$ Hz), 144.4, 172.2; MS (LDI-TOF) m/z [M + H] calcd for $\text{C}_{35}\text{H}_{16}\text{F}_{10}\text{N}_2\text{O}_2\text{H}$ 687.11, found 687.07; IR ν_{max} (thin film)/ cm^{-1} 1626. Anal. Calcd for $\text{C}_{35}\text{H}_{16}\text{F}_{10}\text{N}_2\text{O}_2$: C, 61.23; H, 2.35; N, 4.08. Found: C, 61.52; H, 2.38; N, 4.12.

5,5-Dimethyl-10,15,20-tris(pentafluorophenyl)phlorin (3a).

The reduction of **2a** (281 mg, 0.500 mmol) with NaBH_4 (946 mg, 25.0 mmol) in THF/methanol (40 mL, 3:1) yielding **2a-OH**, immediately followed by condensation with **1d** (156 mg, 0.500 mmol) in the presence of TFA (1.54 mL, 20.0 mmol) in CH_2Cl_2 (200 mL), oxidation with DDQ (166 mg, 0.730 mmol), and filtration of the crude reaction mixture through a pad of silica gel were carried out as described in the literature.^{14,20} Purification of **3a** from the partially purified mixture obtained from the silica pad was refined from our earlier publication,¹⁴ and was carried out as follows. The sample was adsorbed onto neutral alumina (15 g) and purified by chromatography [alumina, CH_2Cl_2 /hexanes (1:4)] affording **3a** (288 mg) that was subsequently crystallized from CH_2Cl_2 /hexanes with gradual evaporation of the CH_2Cl_2 over ~1 h at ~50 °C providing dark purple/green crystals (49%, 206 mg): ^1H NMR (CDCl_3 and $\text{DMSO}-d_6$) and LD-MS analyses were consistent with published values:¹⁴ λ_{abs} (toluene, $\epsilon \times 10^3$) 358 (28.4), 419 (39.8), 438 (45.4), 654 (26.7); λ_{abs} (CHCl_3 , $\epsilon \times 10^3$) 358 (29.2), 416 (41.9), 437 (48.4), 653 (27.7); $^{13}\text{C}\{^1\text{H}\}$ NMR (CDCl_3 , 100 MHz) δ 25.1, 34.8, 91.5, 107.1, 108.3, 121.7, 126.9, 127.6, 131.2, 131.4, 144.2, 154.9 (additional weak signals were present at ~114 ppm and in the region of 135–147 ppm due to carbon atoms of the C_6F_5 substituents).

5-Methyl-5-phenyl-10,15,20-tris(pentafluorophenyl)phlorin (3b). Following a literature procedure,^{14,20} the reduction of **2b** (312 mg, 0.500 mmol) with NaBH_4 (946 mg, 25.0 mmol) in THF/methanol (40 mL, 3:1) afforded the corresponding dicarbinol **2b-OH**, which was used without purification. The reduction reaction was monitored by TLC [alumina, EtOAc/hexanes (1:3)]. The dicarbinol was dried under vacuum for 30 min and then immediately subjected to condensation with **1d** (156 mg, 0.500 mmol) in the presence of TFA (1.54 mL, 20.0 mmol) in CH_2Cl_2 (200 mL) for 15 min at room temperature. Oxidation of the reaction mixture was carried out by the addition of DDQ (166 mg, 0.730 mmol) at room temperature. After 5 min, triethylamine (14 mL, 100 mmol) was added, and the mixture was stirred at room temperature for a further 30 min. The reaction mixture was filtered through a pad of silica gel and eluted with CH_2Cl_2 until the eluent was no longer green. The filtrate was concentrated and adsorbed onto neutral alumina (15 g) and purified by chromatography [alumina, CH_2Cl_2 /hexanes (1:4)] affording **3b** (223 mg) that was subsequently crystallized from CH_2Cl_2 /hexanes with gradual evaporation of the CH_2Cl_2 over ~1 h at ~50 °C providing dark purple/green crystals (24%, 107 mg): λ_{abs} (toluene, $\epsilon \times 10^3$) 357 (27.1), 415 (41.2), 435 (45.0), 651 (25.9); λ_{abs} (CHCl_3 , $\epsilon \times 10^3$) 357 (27.7), 413 (42.0), 434 (46.3), 647 (26.2); ^1H NMR (CDCl_3 , 400 MHz) δ 2.67 (s, 3H), 6.28 (m, 2H), 6.95 (m, 3H), 7.03–7.05 (m, 6H), 7.29 (d, $J =$

4.7 Hz, 2H); ($\text{DMSO}-d_6$, 400 MHz) δ 2.61 (s, 3H), 6.11 (s, 1H), 6.27 (d, $J = 7.2$ Hz, 2H), 6.93 (t, $J = 7.3$ Hz, 1H), 6.98 (s, 2H), 7.02 (d, $J = 7.8$ Hz, 2H), 7.04 (m, 2H), 7.22 (m, 2H), 7.32 (d, $J = 5.0$ Hz, 2H), 7.61 (d, $J = 5.0$ Hz, 2H); $^{13}\text{C}\{^1\text{H}\}$ NMR (CDCl_3 , 100 MHz) δ 29.7, 45.3, 91.3, 106.9, 111.0, 121.5, 125.7, 126.6, 126.9, 127.7, 128.7, 131.4, 132.0, 144.3, 144.8, 155.2 (additional weak signals were present at ~114 ppm and in the region of 135–147 ppm due to carbon atoms of the C_6F_5 substituents); HRMS (ESI-TOF) m/z [M + H] calcd for $\text{C}_{45}\text{H}_{19}\text{F}_{15}\text{N}_4\text{H}$ 901.1443, found 901.1439.

5,5-Diphenyl-10,15,20-tris(pentafluorophenyl)phlorin (3c).

Phlorin **3c** was prepared from **2c** (343 mg, 0.500 mmol) and purified as described above for the preparation of **3b**. Column chromatography [alumina, CH_2Cl_2 /hexanes (1:4)] afforded **3c** (460 mg) that was subsequently crystallized from CH_2Cl_2 /hexanes providing dark purple/green crystals (28%, 135 mg): λ_{abs} (toluene, $\epsilon \times 10^3$) 354 (25.3), 413 (48.1), 431 (49.4), 674 (21.0); λ_{abs} (CHCl_3 , $\epsilon \times 10^3$) 354 (25.9), 412 (47.0), 430 (47.8), 667 (20.9); ^1H NMR (CDCl_3 , 400 MHz) δ 6.48 (d, $J = 4.0$ Hz, 2H), 6.78 (d, $J = 4.0$ Hz, 2H), 6.79 (d, $J = 5.1$ Hz, 2H), 6.98 (m, 4H), 7.06 (d, $J = 5.0$ Hz, 2H), 7.27 (m, 6H); ($\text{DMSO}-d_6$, 400 MHz) δ 6.13 (dd, $J = 1.9, 3.8$ Hz, 2H), 6.85 (d, $J = 6.0$ Hz, 4H), 6.96 (dd, $J = 1.4, 3.7$ Hz, 2H), 7.07 (d, $J = 5.1$ Hz, 2H), 7.28–7.34 (m, 6H), 7.37 (d, $J = 5.0$ Hz, 2H), 7.69 (s, 1H), 8.38 (s, 2H); $^{13}\text{C}\{^1\text{H}\}$ NMR (CDCl_3 , 100 MHz) δ 56.4, 91.6, 107.3, 116.0, 120.9, 127.5, 127.8, 128.0, 128.8, 129.7, 131.8, 132.3, 142.8, 144.8, 156.3 (additional weak signals were present at ~114 ppm and in the region of 135–147 ppm due to carbon atoms of the C_6F_5 substituents); HRMS (ESI-TOF) m/z [M + H] calcd for $\text{C}_{50}\text{H}_{21}\text{F}_{15}\text{N}_4\text{H}$ 963.1599, found 963.1597.

Crystallographic Data. X-ray quality crystals of phlorins **3a–c** were obtained from diffusion of hexane into pyridine solution. Single crystals of **3a–c** were coated in Fomblin oil, mounted on pins, and placed on a goniometer head under a stream of nitrogen cooled to 100 K. For all samples, the frames were integrated with the Bruker SAINT software package using a narrow-frame algorithm. For all three structures, disordered solvent molecules were removed from the structure via the Platon SQUEEZE program. For **3a**, the data were collected on a Bruker SMART APEX CCD-based X-ray diffractometer system equipped with a Mo-target X-ray tube ($\lambda = 0.71073$ Å) operated at 2000 W power. The detector was placed at a distance of 5.009 cm from the crystal. Absorption corrections were carried out using the SADABS program. For **3b** and **3c**, the data were collected on an APEX2 CCD diffractometer with Cu $K\alpha$ radiation ($\lambda = 1.54178$). Data were corrected for absorption effects using the multiscan method and the structure was solved and refined using the Bruker SHELXTL Software Package²⁹ until the final anisotropic full-matrix, least-squares refinement of F^2 converged.

Phlorin Stability Experiments (UV–vis, Uniform Absorbance).¹⁴ In a darkened laboratory, solutions of phlorins **3a–c** were prepared in hexanes, toluene, CH_2Cl_2 , THF, ethyl acetate, acetone, acetonitrile, and methanol. The concentration of each solution was adjusted so that the maximum absorbance of the long wavelength peak (638–679 nm) was ~0.7. UV–vis spectra were recorded in the dark, and then the solutions were exposed to room lights (conventional overhead fluorescent lighting). Spectra were recorded at 15 min, 30 min, 1 h, 1.5 h, 2 h, 4 h, 6 h, 8 h, 1 d, 1.5 d, 2 d, 3 d, 4 d, 5 d, 6 d, 7 d, 8 d, 9 d, 10 d, 11 d, 12 d, 13 d, and 14 d of continuous exposure to room lights. Decomposition of phlorins **3a–c** was inferred from changes in the intensity of the peak at 638–679 nm (longer wavelength peak) and from changes in the intensity of the peak at 426–439 nm (shorter wavelength peak). Data were normalized with respect to the maximum absorbance of the monitored peak prior to exposure to light. Control experiments carried out previously established that phlorin solutions are stable in the absence of light.^{13,14}

Phlorin Stability Experiments (UV–vis, Uniform Concentration).¹⁴ In a darkened laboratory, solutions of phlorins **3a–c** were prepared in toluene, CH_2Cl_2 , THF, and methanol. The concentration of each solution was ~0.025 mM. UV–vis spectra were recorded in the dark, and then the solutions were exposed to room lights, and monitored as described above.

Phlorin Stability Experiments (HPLC, Uniform Concentration).¹⁴ In a darkened lab, solutions of phlorins 3a–c were prepared in toluene, CH₂Cl₂, and THF. The concentration of each solution was ~0.30 mM. The samples were analyzed in the dark by HPLC, and then the solutions were exposed to light (conventional overhead fluorescent lighting). Chromatograms were recorded at 2 h, 4 h, 8 h, 1 d, 1.5 d, 2 d, 3 d, 4 d, 5 d, 6 d, 7 d, 8 d, 9 d, 12 d, 13 d, and 14 d of continuous exposure to room lights. Decomposition of phlorins 3a–c was inferred by a decline in the peak area. HPLC analysis was performed with an injection volume of 1 μ L, a normal-phase silica column (Alltech, Altima, 4.6 mm \times 250 mm), using an isocratic solvent mixture of 95.5% hexanes and 4.5% acetone. The hexanes solvent was 50% water saturated by mixing equal quantities of hexanes and hexanes stored over water. The solvent flow rate was controlled as follows: $T = 0$ –6 min, 1 mL/min; $T = 6$ –7 min, linear increase to 2 mL/min; $T = 7$ –13 min, 2 mL/min; $T = 13$ –14 min, linear decrease to 1 mL/min. Phlorins 3a–c eluted at 8.5, 7.5, and 7.2 min, respectively. Detection was performed at 434 nm (3a–b) and 430 nm (3c).

■ ASSOCIATED CONTENT

● Supporting Information

NMR spectra of diacyldipyrromethanes 2a–c, NMR spectra of phlorins 3a–c, discussion of the partial assignment of ¹H NMR spectra for phlorins 3a–c, UV–vis spectra of phlorins 3a–c, overlaid UV–vis spectra of phlorins 3a–c exposed to light, plots of the absorbance of phlorins 3a–c as a function of time of exposure to light, plots of HPLC peak area of phlorins 3a–c as a function of time of exposure to light, and crystallographic data for phlorins 3a–c. This material is available free of charge via the Internet at <http://pubs.acs.org>.

■ AUTHOR INFORMATION

Corresponding Authors

*E-mail: ziegler@uakron.edu.

*E-mail: ggeier@colgate.edu.

Notes

The authors declare no competing financial interest.

■ ACKNOWLEDGMENTS

Support for this work was provided by the National Science Foundation under Grant No. 0517882 (GRG). High-resolution mass spectra were obtained at the North Carolina State University Department of Chemistry Mass Spectrometry Facility. Funding was obtained from the North Carolina Biotechnology Center and the North Carolina State University Department of Chemistry.

■ REFERENCES

- (1) Sessler, J. L.; Zimmerman, R. S.; Bucher, C.; Kral, V.; Andrioletti, B. *Pure Appl. Chem.* **2001**, *73*, 1041–1057.
- (2) Dehaen, W. *Top. Heterocycl. Chem.* **2010**, *24*, 75–102.
- (3) Aviv-Harel, I.; Gross, Z. *Chem.—Eur. J.* **2009**, *15*, 8382–8394.
- (4) Pistner, A. J.; Yap, G. P. A.; Rosenthal, J. J. *Phys. Chem. C* **2012**, *116*, 16918–16924.
- (5) Ka, J. W.; Lee, C. H. *Tetrahedron Lett.* **2001**, *42*, 4527–4529.
- (6) Hong, S. J.; Ka, J. W.; Won, D. H.; Lee, C. H. *Bull. Korean Chem. Soc.* **2003**, *24*, 661–663.
- (7) Whitlock, H. W.; Oester, M. Y. *J. Am. Chem. Soc.* **1973**, *95*, 5738–5741.
- (8) Woodward, R. B. *Ind. Chim. Belg.* **1962**, *27*, 1293–1308.
- (9) Jeandon, C.; Krattinger, B.; Ruppert, R.; Callot, H. J. *Inorg. Chem.* **2001**, *40*, 3149–3153.
- (10) Setsune, J. –i.; Ikeda, M.; Iida, T.; Kitao, T. *J. Am. Chem. Soc.* **1988**, *110*, 6572–6574.
- (11) Krattinger, B.; Callot, H. J. *Chem. Commun.* **1996**, 1341–1342.

- (12) Krattinger, B.; Callot, H. J. *Eur. J. Chem.* **1999**, 1857–1867.
- (13) LeSaulnier, T. D.; Graham, B. W.; Geier, G. R., III. *Tetrahedron Lett.* **2005**, *46*, 5633–5637.
- (14) O'Brien, A. Y.; McGann, J. P.; Geier, G. R., III. *J. Org. Chem.* **2007**, *72*, 4084–4092.
- (15) Pistner, A. J.; Lutterman, D. A.; Ghidui, M. J.; Ma, Y.-Z.; Rosenthal, J. *J. Am. Chem. Soc.* **2013**, *135*, 6601–6607.
- (16) Littler, B. J.; Miller, M. A.; Hung, C.-H.; Wagner, R. W.; O'Shea, D. F.; Boyle, P. D.; Lindsey, J. S. *J. Org. Chem.* **1999**, *64*, 1391–1396.
- (17) Berube, C. D.; Yazdanbakhsh, M.; Gambarotta, S.; Yap, G. P. A. *Organometallics* **2003**, *22*, 3742–3747.
- (18) Freckmann, D. M. M.; Dube, T.; Berube, C. D.; Gambarotta, S.; Yap, G. P. A. *Organometallics* **2002**, *21*, 1240–1246.
- (19) Laha, J. K.; Dhanalekshmi, S.; Taniguchi, M.; Ambrose, A.; Lindsey, J. S. *Org. Process Res. Dev.* **2003**, *7*, 799–812.
- (20) Rao, P. D.; Dhanalekshmi, S.; Littler, B. J.; Lindsey, J. S. *J. Org. Chem.* **2000**, *65*, 7323–7344.
- (21) Geier, G. R., III; Chick, J. F. B.; Callinan, J. B.; Reid, C. G.; Auguscinski, W. P. *J. Org. Chem.* **2004**, *69*, 4159–4169.
- (22) Geier, G. R., III; Callinan, J. B.; Rao, D. P.; Lindsey, J. S. *J. Porphyrins Phthalocyanines* **2001**, *5*, 810–823.
- (23) Gupta, I.; Fröhlich, R.; Ravikanth, M. *Chem. Commun.* **2006**, 3726–3728.
- (24) Gokulnath, S.; Chandrashekar, T. K. *Org. Lett.* **2008**, *10*, 637–640.
- (25) Higashino, T.; Osuka, A. *Chem.—Asian. J.* **2013**, *8*, 1994–2002.
- (26) Liu, B.; Li, X.; Xu, X.; Stepien, M.; Chmielewski, P. J. *J. Org. Chem.* **2013**, *78*, 1354–1364.
- (27) Gryko, D. T.; Koszarna, B. *Eur. J. Org. Chem.* **2005**, 3314–3318.
- (28) Geier, G. R., III; Grindrod, S. C. *J. Org. Chem.* **2004**, *69*, 6404–6412.
- (29) Sheldrick, G. M. SHELXTL, Crystallographic Software Package, Version 6.10, Bruker-AXS, Madison, WI, 2000.